February 2017
Thesis for Master Degree

Studies on the mechanisms of proteasome inhibitor, boretzomib-induced cell death in CT26 and B16F10 cells.

Graduate School of Chosun University

Department of Medical Science

Yun-Jeong Ahn

Studies on the mechanisms of proteasome inhibitor, boretzomib-induced cell death in CT26 and B16F10 cells.

Proteasome inhibitor, Bortezomib 유도 세포사 기전 연구.

February 24, 2017

Graduate School of Chosun University

Department of Medical Science

Yun-Jeong Ahn

Studies on the mechanisms of proteasome inhibitor, boretzomib-induced cell death in CT26 and B16F10 cells.

Advisor: Prof. Ae Ran Moon

A thesis submitted to the Graduate School of the Chosun University in partial fulfillment of the requirements for the Master of Science

October 2016

Graduate School of Chosun University

Department of Medical Science

Yun-Jeong Ahn

Yun-Jeong Ahn's master thesis

has approved by

Chairman 김 태형 

Committee member 문 애란 

Committee member 한 송이 

November 2016

Graduate school of Chosun University

CONTENTS

LIST OF FIGURES

LIST OF ABBREVIATION

3-MA	3-Methyladenine
ATF 6	Activating transcription factor-6
Bax	Bcl-2-associated x protein
BCA	Bicinchoninic acid
Bim	Bcl-2-like protein 11
BSA	Bovine serum albumin
CHOP	C/EBP homologous protein
DCF-DA	2'7'-Dichlorofluorescin diacetate
DMEM	Dulbecco's Modified Eagel Medium
DR5	Death receptor 5
ER	Endoplasmic reticulum
GADD34	DNA-damage-inducible gene
Bip	Binding immunoglobulin protein, also known 78 kDa glucose-regulated protein (GRP78)
IRE1	Inositol-requiring enzyme
LC3	Microtubule- associated protein 1 light chain 3
MM	Multiple myeloma

NAC	N-acetyl-L-cysteine
NCCD	Nomenclature Committee on Cell Death
O.D.	Optical density
PARP	Poly (ADP-ribose) polymerase
PBS	Phosphate buffered saline
PERK	PKR-like eIF2α kinase, also known as EIF2AK3
p-IRE-1	Phosphorylated IRE-1
p-PERK	Phosphorylated PERK
PVDF	Polyvinylidene fluoride
RCD	Regulated cell death
RPMI	Roswell Park Memorial Institute medium
RT	Room temperature
SDS-PAGE	Sodium dodecyl sulfate-polyacrylamide gel electrophoresis
TBST	Tris-Buffered Saline, 0.1% Tween 20
UPR	Unfolded protein response
UPS	Unfolded protein response,
XBP1	X box-binding protein 1
XTT	2,3-Bis-(2-Methoxy-4-Nitro-5-Sulfophenyl)-2*H*-Tetrazolium-5-Carboxanilid

초 록

Proteasome inhibitor, bortezomib 유도 세포사 기전 연구.

안 윤 정
지 도 교 수 : 문 애 란
조 선 대 학 교 대 학 원
의 과 학 과

Bortezomib은 대부분의 세포에서 apoptosis를 유도하는 것으로 잘 알려진 proteasome inhibitor 이다. Bortezomib에 의한 세포사는 세포 내의 생존신호와 죽음신호에 의해 조절된다고 알려져 있지만, 대부분의 민감성 세포들에서 bortezomib에 의한 세포사 과정은 매우 빠르게 진행되어 세포 내 생존신호가 죽음신호로 전환되는 과정에 대해서는 밝혀진 바 없다. 본 연구는 bortezomib에 의한 세포사에 대하여 중간 정도의 저항성을 나타내는 CT26와 B16F10 세포주를 이용하여 bortezomib에 의한 세포 내 신호 전환을 알아 본 연구 이다. Bortezomib에 의한 세포사에 민감한 BMK 세포주는 10 nM 혹은 50 nM의 bortezomib 존재 시, 24 시간 내에 50% 이상의 세포들이 죽지만, CT26와 B16F10 세포주는 100 nM의 bortezomib을 처리하더라도 24 시간 내에 20% 이하의 세포들 만 죽는 것으로 확인되었다. 하지만, 48 시간이 지나면 거의 모든 세포들이 죽게 되는 것으로 보아 24 시간 내에는 세포의 생존신호가 작동하는 것으로 여겨졌다. proteasome inhibition 후 작동하는 것으로 알려진

endoplasmic reticulum (ER) stress 반응과 autophagy가 CT26와 B16F10 세포주에서도 활성화됨을 immunoblotting analysis를 통해 확인하였다. ER stress 반응과 autophagy가 생존신호로 역할을 하는지 확인하기 위하여 ER stress response 억제제인 4μ8C (IRE-1 inhibitor), GSK2606414 (PERK inhibitor) 또는 Salubrinal (eIF2α inhibitor)와 autophagy 억제제인 bafilomycin A1 (BfA) 또는 3-methyl adenine (3-MA)를 각각 bortezomib과 함께 처리한 후 세포사를 확인한 결과 세포사가 증가함을 확인하였다. 대표적인 죽음신호인 caspases는 12 시간 이후부터 활성화하기 시작하여 24 시간이 지나면 최고조에 달하는 것으로 보인다. Caspase 억제제에 의한 세포사 억제를 확인하였지만 세포사는 완벽히 억제되지 않았으며, 또 다른 죽음신호인 활성산소종의 증가를 확인한 결과 8시간 이후부터 증가하는 것을 확인했다. 활성산소종을 감소시키는 NAC과 caspase 억제제를 동시에 처리하였을 경우 세포사는 더 많이 감소하는 것을 확인하였다. 또한 NAC에 의해 활성산소종이 감소하면 caspase의 활성 또한 감소하는 것을 확인하였다. 이러한 결과들을 종합하여, bortezomib 처리 후 세포의 생존신호와 죽음신호의 변화를 시간 별로 확인해볼 수 있었다. CT26 세포주에서는 생존신호가 죽음신호로 변환되는 conversion model이, 그리고 B16F10 세포주에서는 생존신호가 죽음신호와 경쟁하다가 죽음신호로 변환되는 competition model과 부합하는 것을 확인하였다.

I. Introduction

Proteasome is a protein complex involved in degradation of unneeded proteins that are tagged ubiquitin. Functional proteasome is essential for maintenance of cell homeostasis, proliferation and survival. Functional proteasome is also important in cancer, because some cancer cells regulate degradation of proteins such as cell cycle regulatory proteins (e.g., p21, p27) or cell survival proteins (e.g., IκB) in order to create cancer-specific microenvironment [1]. Several proteasome inhibitors have been studied and developed as anti-cancer drugs in this context. Proteasome inhibition facilitates accumulation of unfolded or misfolded proteins, subsequently induces endoplasmic reticulum (ER) stress and unfolded protein response (UPR) to remove unfolded or misfolded proteins [2, 3]. After accumulation of unfolded or misfolded proteins in ER lumen, three major proteins, PKR-like eIF2α kinase (PERK, also known as EIF2AK3), activating transcription factor-6 (ATF 6), and inositol-requiring enzyme (IRE1), are activated by dissociation of 78 kDa glucose-regulated protein (GRP78) [4]. To reduce accumulation of unfolded or misfolded proteins, cap-dependent translation is blocked and only specific proteins are translated, like as ATF4 and C/EBP homologous protein (CHOP) by phosphorylated eIF2α through PERK activation [5]. UPR is feedback regulated after expression of growth-arrest and

DNA-damage-inducible gene (GADD34) and $P58^{IPK}$, induced by CHOP and X box-binding protein 1 (XBP1), respectively [5, 6]. Although UPR is a mechanism for survival, pro-apoptotic proteins are increased by sustained ER stress; resulting in cell death [7-9].

MG-132 is the first developed proteasome inhibitor and inhibits 20S core site in proteasome. However, MG-132 is not adequate for cancer therapy because it has a non-specific binding activity and is quickly dissociated from proteasomes. Bortezomib (PS-341 or Velcade®) is a reversible 26S proteasome inhibitor and the first FDA (food and drug administration)-approved drug for multiple myeloma in U.S [10-12]. Bortezomib induces ER stress and cell cycle arrest [13-15], or apoptosis in almost all cells [16, 17] but also autophagic cell death in proliferating human endothelial cells [18]. Although bortezomib has been known as an inducer of ER stress-mediated cell death and used or tried in specific cancer treatment [19-26], some cancer cells are resistant to bortezomib-induced cell death.

Most of studies about bortezomib-induced cell death have been examined using susceptible cells or genetically modified cells [27]. Although researchers had been referred to life-to-death signal switch, the signal switch would have happened too fast to discriminate pro-survival from pro-apoptosis signals in susceptible cells. In this thesis, I investigated intracellular signal switching mechanism in CT26 cells and B16F10 cells,

which are moderately resistant to bortezomib-induced cell death. Less than 20% of cells were dead within 24 hours after bortezomib treatment, in which ER stress response and autophagy were processed. Cells were dose-dependently dead within 36 and 48 hours after bortezomib treatment due to ROS increase and caspase activation.

II. Materials and Methods

1. Materials

1.1. Cells

BMK (baby mouse kidney), CT26 (mouse colon cancer), B16F10 (mouse melanoma cancer), A549 (human lung carcinoma) and HeLa (human cervical cancer) were obtained from Korean Cell Line Bank (Deajeon, Korea).

1.2. Chemicals

To this study, five proteasome inhibitors (bortezomib, ixazomib, carfilzomib, oprozomib and MG-132) were from Selleckchem (Huston, TX, USA). For cell culture Dulbecco's Modified Eagel Medium (DMEM) and RosIll Park Memorial Institute medium (RPMI) 1640 were obtained from Thermo Scientific (Pittsburg, PA, USA), Fetal Bovine Serum from Capricorn Scientific (Ebsdorfergrund, Germany), 1% Penicillin-streptomycin from Thermo Scientific, Ciprofloxacin from Sigma-Aldrich (St. Louis, MO, USA) and Gentamycin from Duchefa Biochemie (Haarlem, Netherlands). To test cell viability and inhibition assay, XTT (2,3-Bis-(2-Methoxy-4-Nitro-5-Sulfophenyl)-2*H*-Tetrazolium-5-

Carboxanilide) solution was from Promega (Madison, WI, USA), z-VAD-fmk was from Adooq z-DEVD-fmk, z-IETD-fmk and z-LEHD-fmk were from R&D system (Minneapolis, MN, USA), 3-Methyladenine (3-MA) was from Invivogen (San Diego, CA, USA), Bafilomycin A (BfA) was from Biovision (Milpitas, CA, USA) and N-acetyl-L-cysteine (NAC) and 2'7'-Dichlorofluorescin diacetate (DCF-DA) were from Sigma-Aldrich.

1.3 Antibodies

Anti-Caspase-3 (9662), Anti-Caspase-9 (9508), Anti-human Caspase-8 (9746), Anti-Beclin-1 (3495), Anti-Atg5 (12994), Anti-CHOP (2895) and Anti-GRP78/Bip (3177) antibodies are obtained from Cell Signalling (Danvers, MA, USA), Anti-mouse Caspase-8 (ALX-804-447) and Anti-ATF6 (ALX-804-381) antibodies are obtained from EnZo Life Sciences (Farmingdale, NY, USA), Anti-LC3 (GTX17380) antibody is from GenTex (Irvine, CA, USA), Anti-phosphorylated-PERK (sc-3257) antibody is from Santa Cruz Biothechnology (Dallas, TX, USA), Anti-phosphorylated-IRE1 (ab48187) antibody is from Abcam (Cambridge, MA, USA) and Anti-Actin (MAB1501) antibody is from Millipore (Thermo Scientific).

2. Methods

2.1 Cell death assay

2.1.1 Cell culture

BMK, CT26, B16F10 and HeLa cells were cultured in DMEM media and A549 cells were cultured using RPMI1640 media, those media were supplemented with 10% FBS, 1% penicillin-streptomycin, Ciprofloxacin, and Gentamycin in 5% CO_2 at 37℃.

2.1.2 XTT assay

Several kinds of proteasome inhibitors, ranging from 6.25 nM to 200 nM were prepared after serial dilution. Cells ($2X10^4$ cells/well) were seeded into 96-well plate (SPLifesience, Gyeonggi-do, Korea) and cultured overnight. Various amounts of proteasome inhibitors were added into cells and cultured for appropriate time periods. Cell medium was replaced with phenol-red free DMEM containing XTT. After 1.5-hour incubation, optical density (O.D.) was measured using Infinite M200 (Tecan, Männedorf, Switzerland) at 490 nm. Viability was calculated on the basis of O.D. of untreated control as 100%.

2.1.3. Addition of cell death inhibitors

CT26 cells (2X10^4 cells/well) were cultured in 24-well plate (SPLifesience) and treated with 100 nM of bortezomib. After 8 hours of the bortezomib treatment, cells were treated with various cell death inhibitors; z-VAD-fmk, pan-caspase inhibitor; Bafilomycin A, autophagy inhibitor; NAC, ROS scavenger. After additional 24-hours incubation, both suspended and attached cells were harvested and centrifuged using high speed centrifuge (Beckman Counlter, Chaska, MN, USA) at 4,000 rpm for 5 minutes. Thereafter, the supernatant was discarded and the pellet was dissolved in 0.1% trypan blue solution and stained for 2 minutes at 37℃. Live cells were counted using hemocytometer.

2.2 Immunoblotting analysis

2.2.1 Preparation of cell lysates

For immunoblotting analysis, cell lysates were prepared after 100 nM of bortezomib treatment for 6 hours, 12 hours, 24 hours or 48 hours. Briefly, both of attached and suspended cells were harvested using cell scraper and centrifuged at 8,000 rpm for 5 minutes. Cells were lysed with RIPA buffer (50 mM Tris-HCl (pH 7.4), 1% NP-40, 0.5% sodium deoxycholate, 0.1% sodium dodecyl sulfate (SDS), 150 mM NaCl and 2 mM EDTA) supplemented with phosphatase inhibitor cocktails-Ⅰ, -Ⅱ (Sigma) and mixed

thoroughly. The lysed cells were incubated on ice for 10 minutes and then, lysates were obtained by centrifugation at 12,000 rpm 10 minutes. Cell lysates were stored at -20℃.

2.2.2 Protein quantification

Proteins present in each cell lysate were quantified through BCA (bicinchoninic acid) assay (Thermo scientific). Bovine serum albumin (BSA) was used as a standard protein for BCA assay. Serially diluted standard protein solutions and cell lysates were filled in 96-well. After addition of 200 μl of BCA solution mixture (solution A: solution B = 1:50), the plates were incubated at 37℃ for 15 minutes. O.D. was measured at using Infinite M200 (Tecan) and protein concentration was calculated using standard curve.

2.2.3 Gel electrophoresis

Appropriate amounts of cell lysates were mixed with protein loading buffer (final concentration: 50 mM Tris-HCl (pH 6.8), 2% SDS, 10% glycerol, 1% β-mercaptoethanol, 12.5 mM EDTA and 0.02% bromophenol blue) and boiled for 10 minutes. Immediately after the boiling, cell lysates were incubated on ice for 10 minutes. Cell lysates were loaded onto appropriate concentrations of sodium dodecyl sulfate-polyacrylamide gel electrophoresis (SDS-PAGE) gel and then electrophoresed.

2.2.4 Immunoblotting analysis

After gel electrophoresis, SDS-PAGE gels were assembled into transfer cassettes in the orders of sponge-3mm paper-SDS PAGE gel- polyvinylidene fluoride (PVDF) membrane-3mm paper-sponge. To transfer proteins, gel electrophoresis kit equipped with transfer cassettes was run at 100 mA for overnight or 300 mA for 3 hours. The PVDF membranes were immersed with TBST (5 mM Tris-cl (pH 7.6), 15 mM sodium chloride (NaCl), 0.1% Tween 20) buffer containing 2.5% or 5% skim milk at room temperature (RT) for 1 hour. After removal of TBST buffer, appropriately diluted primary antibody was added into the membranes and incubated as follows; anti-caspase 3 antibody (1:2000) at RT for 3 hours; anti-caspase 8, anti-caspase 9, anti-LC3, anti-GRP78/Bip, anti-phosphorylated PERK, anti-phosphorylated IRE1, anti-ATF6, and anti-CHOP (1:1000) at 4℃ for overnight. After incubation, membranes were washed three times with 0.05% TBST for 10 minutes each. Appropriate secondary antibodies were added and incubated for 1 hour at RT. Membranes were washed four times with 0.05% TBST for 10 minutes each and immuno-reactive bands were detected using PowerOpti-ECL™ solution (Animal Genetics, Suweon, Korea).

2.3 ROS assay

Cells ($2X10^4$ cells/well) were cultured in 12-well plates (SPLifescience) overnight. Bortezomib was treated for 8, 16, 24, or 32 hours, and then cells were washed twice with phosphate buffered saline (PBS). After addition of 2 μM of DCF-DA, cells were incubated for 30 minutes at 37℃ in the dark. Fluorescence was analyzed at 266 nm/545 nm as excitation/emission wavelengths using fluorometric plate reader (Luminescence Spectrophotometer LS S5, Perkin Elmer, Waltham, MA, USA) using FL WinLab program. Cells were microscopically observed by fluorescence microscopy (Olympus 1X71) using DP2-BSW program with 0.8-seconds exposure. Relative ROS generation was calculated on the basis of XTT value.

2.4. Enzymatic activity assay of caspase 3 and caspase 8

Enzymatic activity of Caspase-3 or Caspase-8 was assayed using Caspase-3 and Capase-8 colorimetric assay kit (R&D system). CT26 and B16F10 cells were treated with bortezomib in the presence or absence of NAC. Cells were harvested using lysis buffer in the kit and centrifuge at 12,000 rpm for 10 minutes. Amounts of proteins were quantified using BCA assay and concentrations were adjusted to 2 mg/ml using lysis buffer. After mixing with 2 × reaction buffer in the kit with 1:1 ratio, 50 μl of cell lysates was added

into 96-well plate. For reaction, 5 μl of substrate solution in the kit was added into each well and the plates were incubated at 37℃ for 1 hour. O.D. was measured by Infinite M200 (Tecan) at 405 nm.

III. Results

1. Classification of cells according to the responsiveness to bortezomib.

To identify signal switching mechanism in proteasome inhibitor-induced cell death, cells were classified depending on the responsiveness to bortezomib-induced cell death. BMK, CT26, B16F10, A549 and HeLa cells were treated with 100 nM of bortezomib and cell deaths were measured using XTT assay. Figure 1 showed that CT26 and B16F10 were resistant to bortezomib-induced cell death only within 24 hours. BMK cells were susceptible to bortezomib-induced cell death because over 50% of cells were dead within 24 hours. HeLa and A549 cells were seemed to be highly resistant since approximately 10% of cells were dead even after 32 hours. From this result, CT26 and B16F10 cells appeared to be adequate to identify signal switching mechanism because their cell deaths were seemed to be inhibited within 24 hours and induced after 24 hours. To investigate the responsiveness of CT26 and B16F10 cells to other proteasome inhibitors, carfilzomib, MG-132, bortezomib, ixazomib or oprozomib was treated and cell deaths were analyzed. Cytotoxicity of oprozomib or MG-132 on CT26 was relatively lower than bortezomib,

ixazomib and carfilzomib (Figure 2). To investigate process of cell death by bortezomib, cell death rates were examined in time-dependent and dose-dependent manners using CT26 and B16F10 cells. Cells were treated with bortezomib ranging from 6.25 nM to 200 nM and cell death was analyzed in time-dependent manner. Cell death was inhibited within 24 hours even in 200 nM of bortezomib treatment but significantly increased within 24 and 48 hours. It could be suggested that survival signals were activated within 24 hours to inhibit cell death. (Figure 3 A, B).

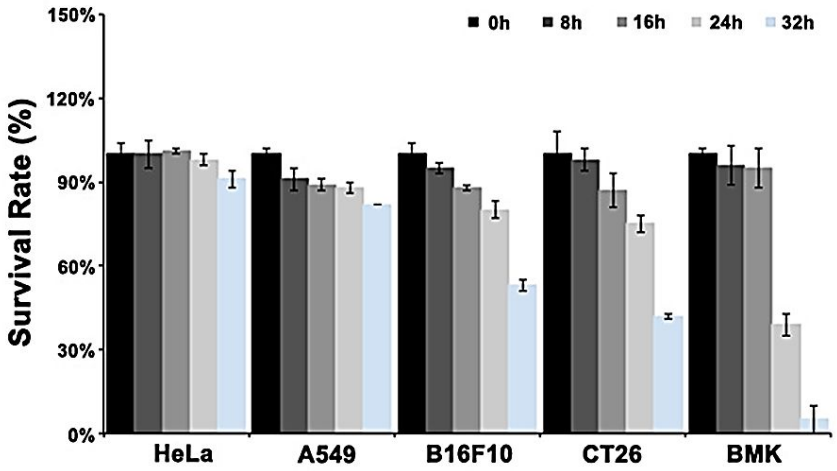

Figure 1. Responsiveness to bortezomib in various cells

Cells (1×10^4 cell/ well) were seeded into 96-well plate a day before bortezomib treatment. After the bortezomib treatment, cell survival rates were examined in time-dependent manner by XTT assay. Error bars meant standard deviation.

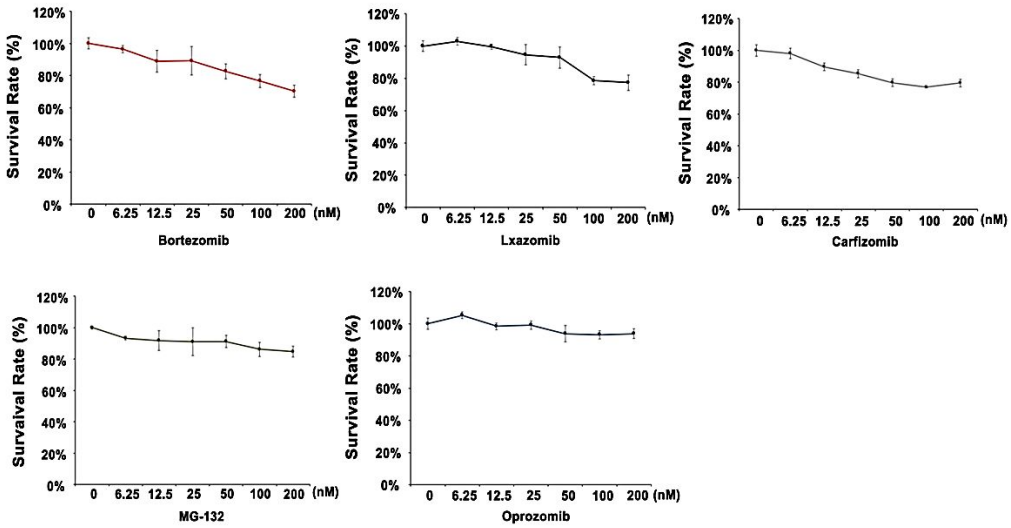

Figure 2. Responsiveness of CT26 cells to various proteasome inhibitors

Cells (1×10^4 cell/ well) were seeded into 96-well plate a day before the treatment. Various amounts of proteasome inhibitors, bortezomib, ixazomib, carfilzomib, oprozomib or MG-132, were treated into CT26 cells for 24 hours. Survival rate was analyzed using XTT assay. Error bars meant standard deviation.

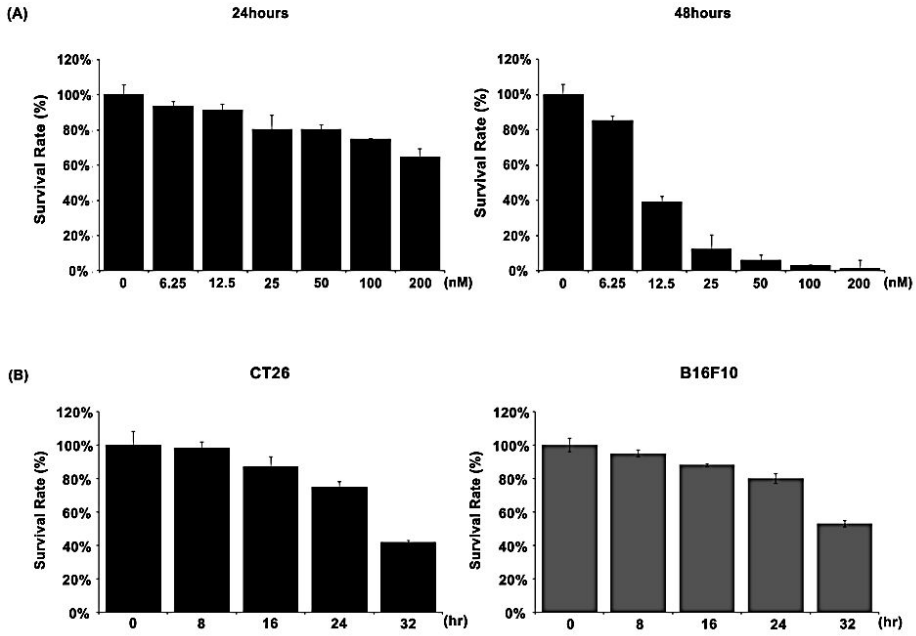

Figure 3. Cell death assay in CT26 and B16F10 cells after bortezomib treatment

Cells (1×10^4 cell/ well) were seeded into 96-well plate a day before bortezomib treatment. (A) Indicated amounts of bortezomib were treated into CT26 cells and cell survival rates were measured uxing XTT assay. (B) After the treatment of bortezomib (100 nM) into CT26 and B16F10 cells, cell survival rate was determined time-dependently using XTT assay. Error bar means Standard deviation.

2. Death signals in CT26 and B16F10 cells.

Since apoptosis has been known cell death mechanism by proteasome inhibition [10, 25, 26], apoptotic signals were assayed in bortezomib-treated CT26 and B16F10 cells in time-dependent manner. Cleavages of caspase 9 and poly (ADP-ribose) polymerase (PARP) were detected from 6 hours in CT26 cells (Figure 4A). Cleaved caspase 3 and 8 were detected from 24 hours in CT26 cells but cleaved caspase 8 were not significant in B16F10 cells. To confirm whether caspase 3 or 8 was activated, enzymatic activities of caspase 3 or 8 were measured (Figure 4B). Enzymatic activities of caspase 3 and 8 were increased from 6 hours and reached about 15- or 5-fold at 24 hours in CT26 cells, respectively. However, only caspase 3 was activated from 24 hours in B16F10 cells. Caspase activation seemed to be enough to induce cell death at 24 hours after bortezomib treatment but cells were not dead. As the increase of cell death did not coincide with caspase activation, it became necessary to examine whether caspases would be involved in bortezomib-induced cell death using various caspase inhibitors. Cell death was partially inhibited by addition of z-VAD-fmk; pan-caspase inhibitor, z-DEVD-fmk; caspase 3 specific inhibitor, or z-IETD-fmk; caspase 8 specific inhibitor but not caspase 9 specific inhibitor, z-LEHD-fmk in CT26 cells (Figure 5).

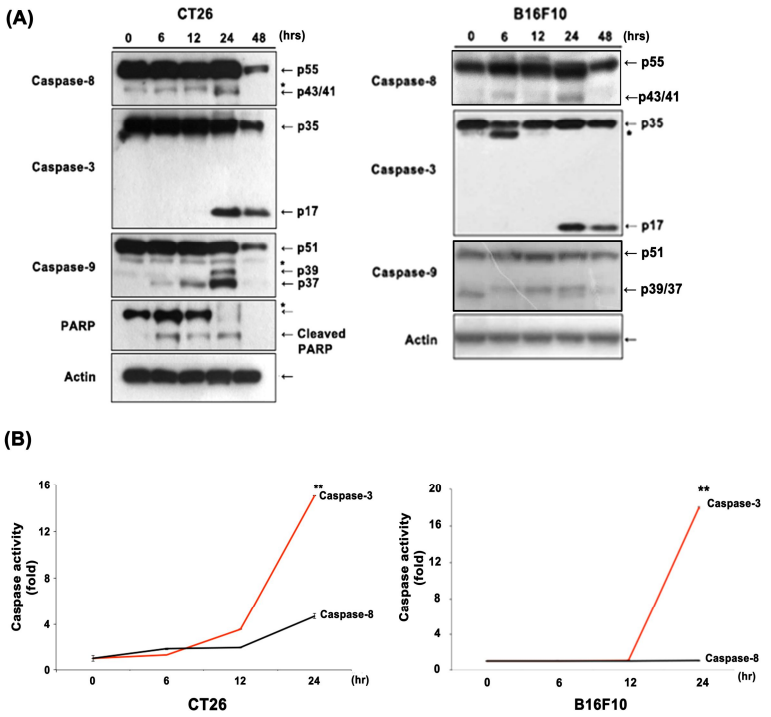

Figure 4.Caspase-3 and/or caspase-8 activation in bortezomib-treated CT26 and B16F10 cells

(A) Cell lysates were prepared from CT26 and B16F10 after 100 nM of bortezomib treatment in time-dependent manner. Immunoblotting analysis was performed using antibodies against indicating proteins. Reactive bands were indicated by arrow, and asterisk showed nonspecific bands. Actin as a protein loading control was detected using anti-actin antibody. (B) Enzymatic activities of caspase 3 or 8 were assayed using CT26 and B16F10 cell lysates using caspase assay kit described in 'Methods'. n=3; **P<0.01; Student's t test between the results in 12 hours and 24 hours..

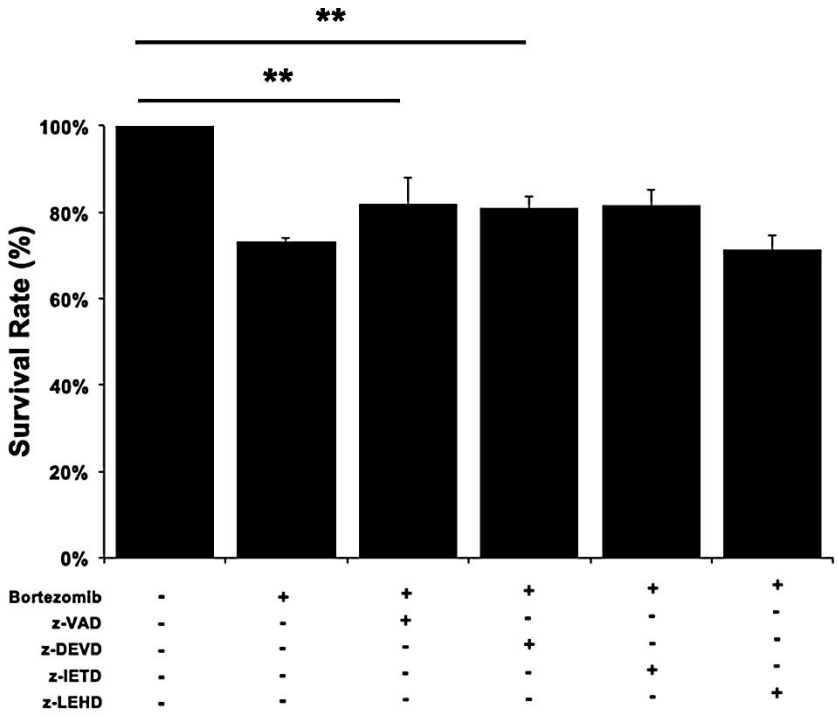

Figure 5. Cell death assay after addition of casapse inhibitors

To identify whether activated caspases were involved in bortezomib-induced cell death, cell survival rates were measured after the co-treatment of caspase inhibitors with bortezomib in CT26 cells; z-VAD-fmk, pan-caspase inhibitor; z-DEVD-fmk, caspase 3 specific inhibitor; z-IETD-fmk, caspase 8 specific inhibitor; z-LEHD-fmk, caspase 9 specific inhibitor. Error bars meant standard deviation. n=3; **P<0.01; Student's t test

3. Survival signals in CT26 and B16F10 cells.

Considering that increase of cell death was not synchronized with caspase activation, whether anti-apoptotic proteins or pro-survival signals were activated within 24 hours, was investigated. Mcl-1 was increased between 6 hours and 24 hours but not detected at 48 hours (Figure 6). Expressions of XIAP, cIAP1, and cIAP2 were not regulated by bortezomib (data not shown). Since autophagy is induced by, or with ER stress response [27-29] and shows cytoprotective roles in various conditions [28, 30, 31], cell death rates were analyzed after addition of autophagy inhibitors: bafilomycin A1 (BfA) or 3-methyl adenine (3-MA) (Figure 8). Cell death rates were increased by BfA or 3-MA, suggesting that autophagy should be cytoprotective in bortezomib-treated cells. To investigate time-dependent progress of ER stress response and autophagy signaling, profiling of ER stress or autophagy related proteins was performed after addition of bortezomib (Figure 7, 10). Three ER membrane proteins, PERK, IRE-1, and ATF6, were activated or increased only within 24 hours after bortezomib treatment in CT26 and B16F10 cells, when cell death was hardly detected. Phosphorylated PERK (p-PERK) and phosphorylated IRE-1 (p-IRE-1) were detected between 6 and 12 hours but not detected at 24 hours after bortezomib treatment in CT26 cells. Expression levels of ATF6 was increased at 6 hours and returned to basal level 24 hours after bortezomib treatment in both cells. Autophagy

seemed to be induced after ER stress response, according to the result that cleaved LC3 (microtubule- associated protein 1 light chain 3) and LC3-Ⅱ was detected from 12 hours. Initiation of autophagy would be reduced around 48 hours because beclin-1 and Atg5 were decreased between 24 and 48 hours in B16F10 or CT26 cells, respectively. Cell death rates was correlated with decrease of beclin-1 and Atg5 in CT26 and B16F10 cells.

Since autophagy was survival signal and followed by ER stress response, whether cell death could be regulated by ER stress inhibition was examined. CT26 cells were treated with bortezomib and ER stress inhibitors, IRE-1 inhibitor (4μ8C), PERK inhibitor (GSK2606414) or eIF2α inhibitor (Salubrinal) for 24 hours. In Figure 9, cell death rates were increased after addition ER stress response inhibitors. These results showed that ER stress response and autophagy were survival signals in bortezomib-treated cells (Figure 11).

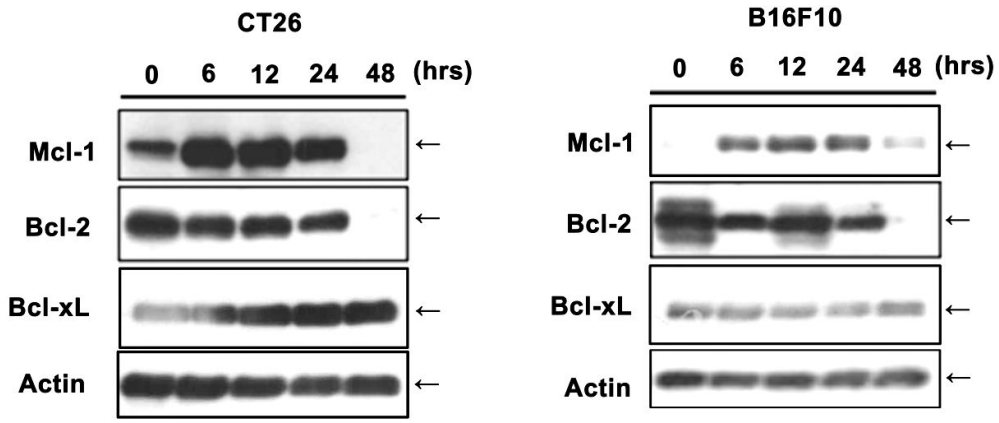

Figure 6. Anti-apoptotic proteins in bortezomib-treated CT26 and B16F10 cells

Cell lysates were prepared from CT26 and B16F10 after 100 nM of bortezomib treatment in time-dependent manner. Immunoblotting analysis was performed using antibodies against indicating proteins. Reactive bands were indicated by arrow, and asterisk showed nonspecific bands. Actin as a protein loading control was detected using anti-actin antibody.

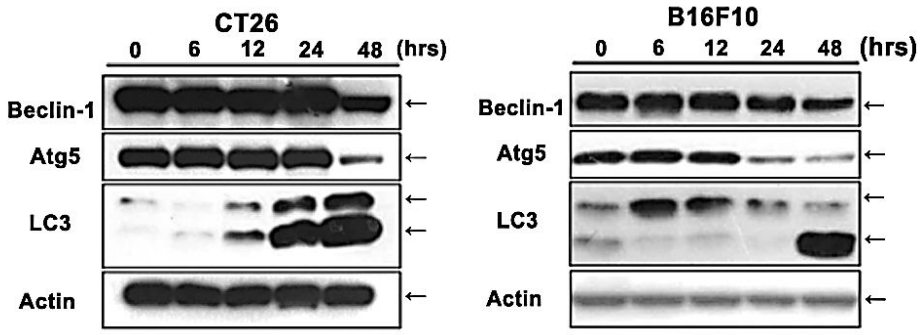

Figure 7. Autophagy signals in bortezomib-treated CT26 and B16F10 cells

After 100 nM of bortezomib treatment, cell lysates were prepared in time-dependent manner. To examine autophagy process, autophagy related proteins were detected using immunoblotting analysis. Reactive bands were indicated by arrow. Actin as a protein loading control was detected using anti-actin antibody.

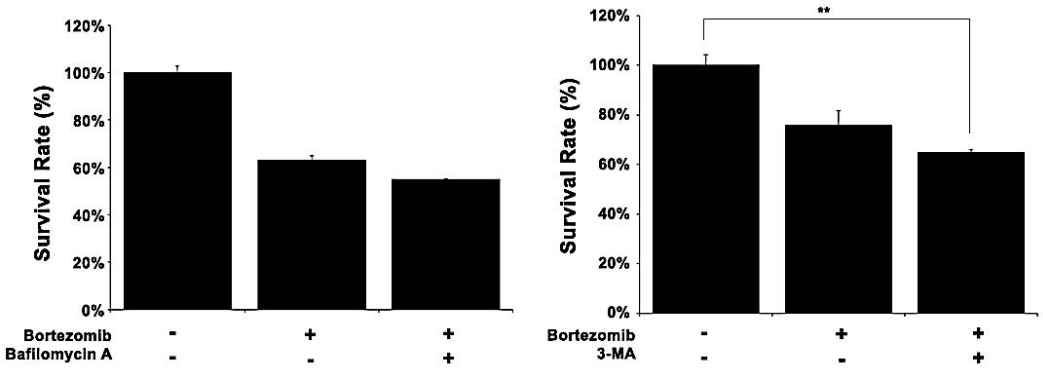

Figure 8. Cell dath assay after addition of autophagy inhibitors

Cells (1×10^4 cell/ well) were seeded into 96-well plate a day before bortezomib treatment. Cells were treated with 100 nM of bortezomib with or without autophagy inhibitors; 20 nM of BfA; 5 mM of 3-MA. After 24 hours, cell survival rates were measured using XTT assay. Error bar meant standard deviation. n=3; **P<0.01; Student's t test.

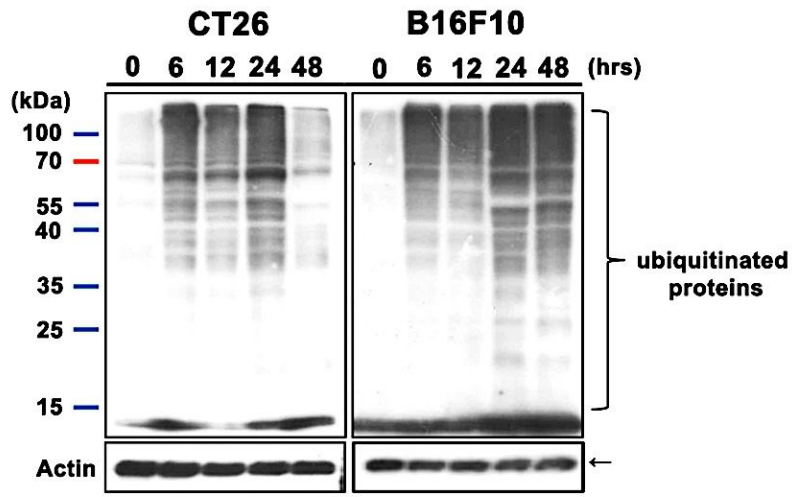

Figure 9. Accumulation of ubiquitinated proteins in bortezomib-treated CT26 and B16F10 cells

After 100 nM of bortezomib treatment, cell lysates were prepared. Ubiquitinated proteins were detected in each cell lysate using anti-ubiquitin antibody as described in 'Methods'. Actin as a protein loading control was detected using anti-actin antibody.

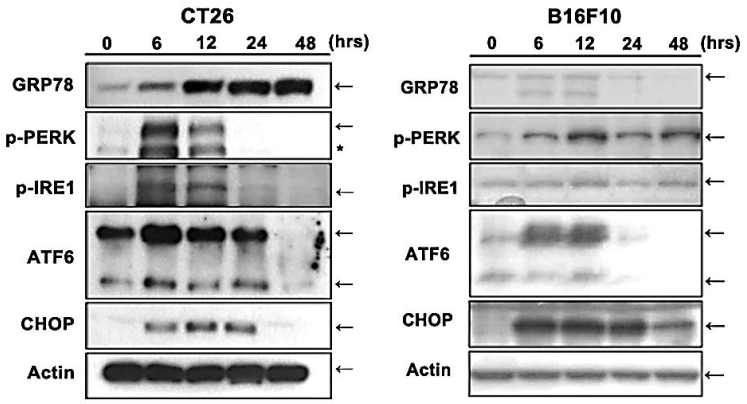

Figure 10. ER stress response in bortezomib-treated CT26 and B16F10 cells

After 100 nM of bortezomib treatment, cell lysates were prepared in time-dependent manner. To examine ER stress response, ER stress related proteins were detected using immunoblotting analysis. Reactive bands were indicated by arrow, and asterisk showed nonspecific bands. Actin as a protein loading control was detected using anti-actin antibody.

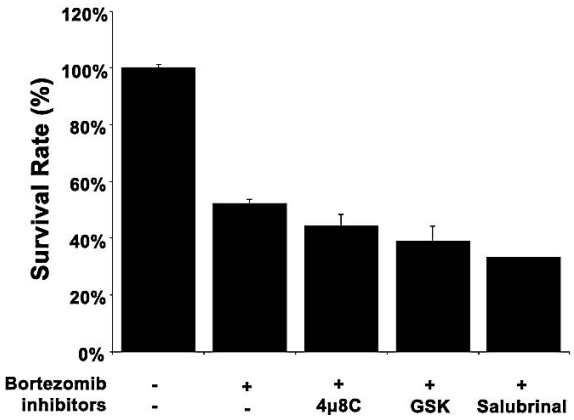

Figure 11. Cell death assay after addition of ER stress response inhibitors

Cells (1×10^4 cell/ well) were seeded into 96-well plate a day before bortezomib treatment. Cells were treated with 100 nM of bortezomib with or without ER stress response inhibitors; 10 nM of 4μ8C; 30 nM of GSK2606414; 30 μM of salubrinal. After 24 hours, cell survival rates were measured using XTT assay. Error bar meant standard deviation. n=3; *P<0.05; **P<0.01; Student's t test. Continued next page.

4. An additional pro-death signal.

Because cell death was partially decreased by caspase inhibitor (Figure 5), whether additional pro-death signal was involved in bortezomib-induced cell death was examined. Since reactive oxygen species (ROS) are known to be increased by ER stress and to induce caspase-independent apoptosis [32], ROS assay was performed using 2',7'-dichlorofluorescein diacetate (DCF-DA) to investigate additional pro-death signal. ROS was increased from 8 hours and reached about two-fold at 24 hours in CT26 and B16F10 cells (Figure 12). To test if bortezomib-induced cell death was stimulated by ROS, cell death rate was assayed in bortezomib-pretreated CT26 and B16F10 cells after addition of ROS scavenger, N-acetyl-L-cysteine (NAC). Cell death was slightly inhibited by NAC and additively inhibited in the presence of z-VAD-fmk (Figure 13). Because time-dependent increase of ROS appeared similar to the results of caspase activation, caspase activities were assayed after addition of NAC into bortezomib-treated CT26 and B16F10 cells to identify whether ROS would affect caspase activation. Approximately 50% of caspase 3 activity was reduced but caspase 8 activity was not affected by addition of NAC in both cells (Figure 14). It could be suggested that cell death was processed by ROS and activated caspase 3 and/or 8 in bortezomib-treated CT26 and B16F10 cells, in which ROS could be one of the stimulating factors for caspase 3 activation.

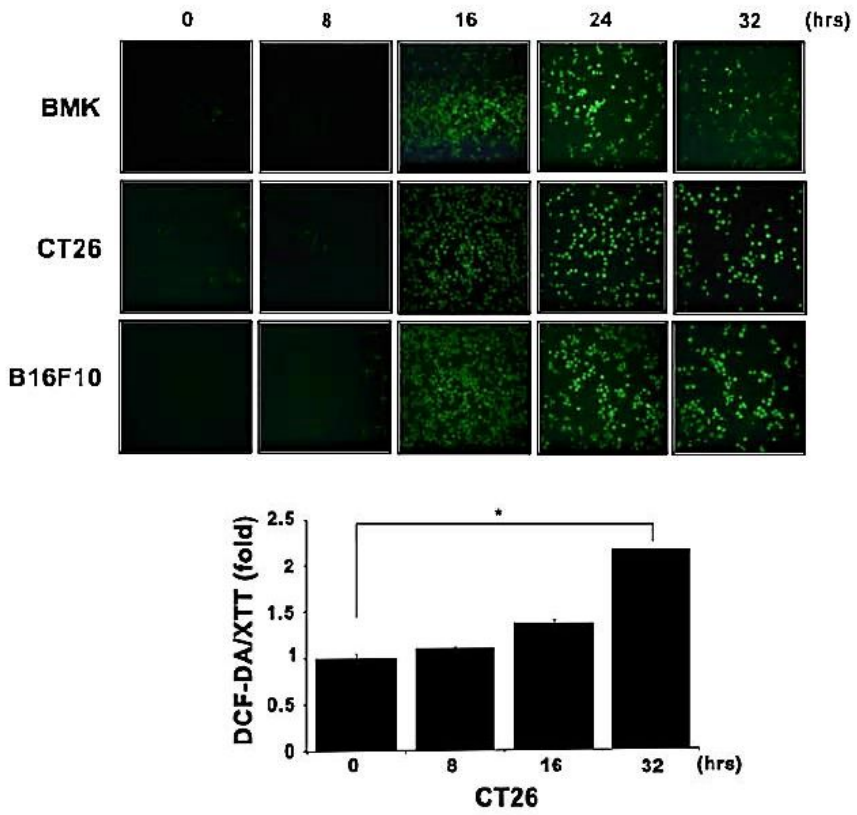

Figure 12. Reactive oxygen species (ROS) generation in bortezomib-treated CT26 and B16F10 cells

Cells (1×10^4 cells/ well) were seeded into black 96-well plate a day before bortezomib treatment. (A) DCF-DA (2 μM) was added into CT26 or B16F10 cells at 8, 16, and 24 hours after 100 nM of bortezomib treatment and cells were incubated for 30 minutes at 37℃. Extents of fluorescence were measured at 266 nm/545 nm as excitation/emission wavelengths using Luminescence Spectrophotometer LS S5 (Perkin Elmer). n=3; *P<0.05; Student's t test.

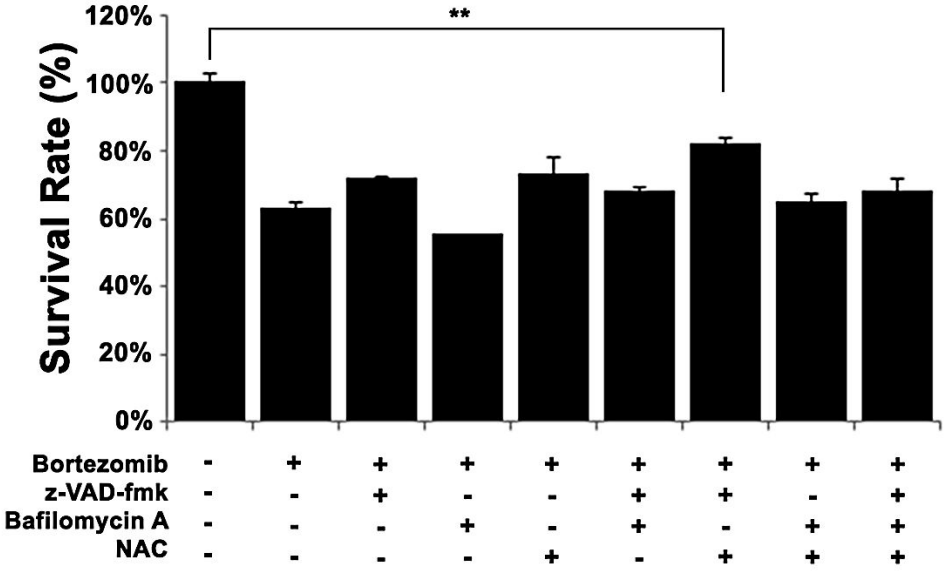

Figure 13. Cell death assay after addition of caspase inhibitor and ROS scavenger

Cells (1×10^4 cells/ well) were seeded into black 96-well plate a day before bortezomib treatment. BfA or z-VAD-fmk was treated with 100 nM of bortezomib. NAC (1mM) was treated 8 hours after 100 nM of bortezomib treatment. Cell death was examined 24 hours after bortezomib treatment by trypan blue exclusion experiments. n=3; **P<0.01; Student's t test.

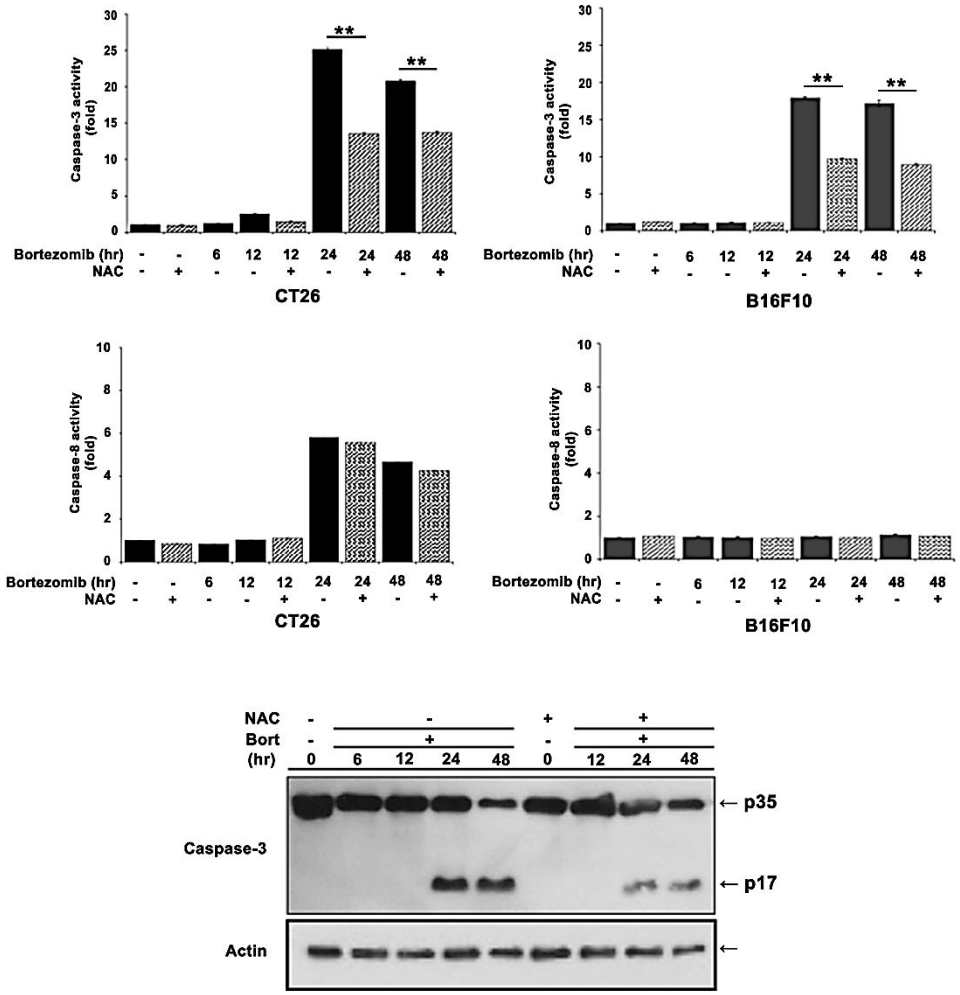

Figure 14. Caspase-3 activation after NAC treatment

NAC (1mM) was treated 8 hours after 100 nM of bortezomib treatment. Cell lysates were prepared in time-dependent manner and activations of caspase 3 and 8 were analyzed using immunoblotting analysis and enzymatic assay. n=3; *P<0.05; Student's t test.

5. Regulation of cell death in CT26 and B16F10 cells.

Previously, two models have been suggested to explain mechanism of regulated cell death (RCD) and adaptive stress responses [33]. In conversion model, RCD-inhibitory signals are ceased and substituted with RCD-promoting signals. Competitive model postulates that RCD-inhibitory signals and RCD-promoting signals are co-existent and counteractive to each other. To identify that bortezomib-induced cell death could be related to one of the two models, relationships of ER stress response, autophagy, ROS, or caspase activation and cell death were analyzed. Each band intensity of immunoblotting was measured using Image J program and relative intensities were shown in Figure 15. Increase of cell death was inversely related with decrease of ER stress response and autophagy, referred to RCD-inhibitory signals. Caspase activation and increase of ROS coincided with cell death. From this analysis, signal switching mechanism in CT26 cells was close to conversion model and that in B16 F10 cells was to competitive model after bortezomib treatment.

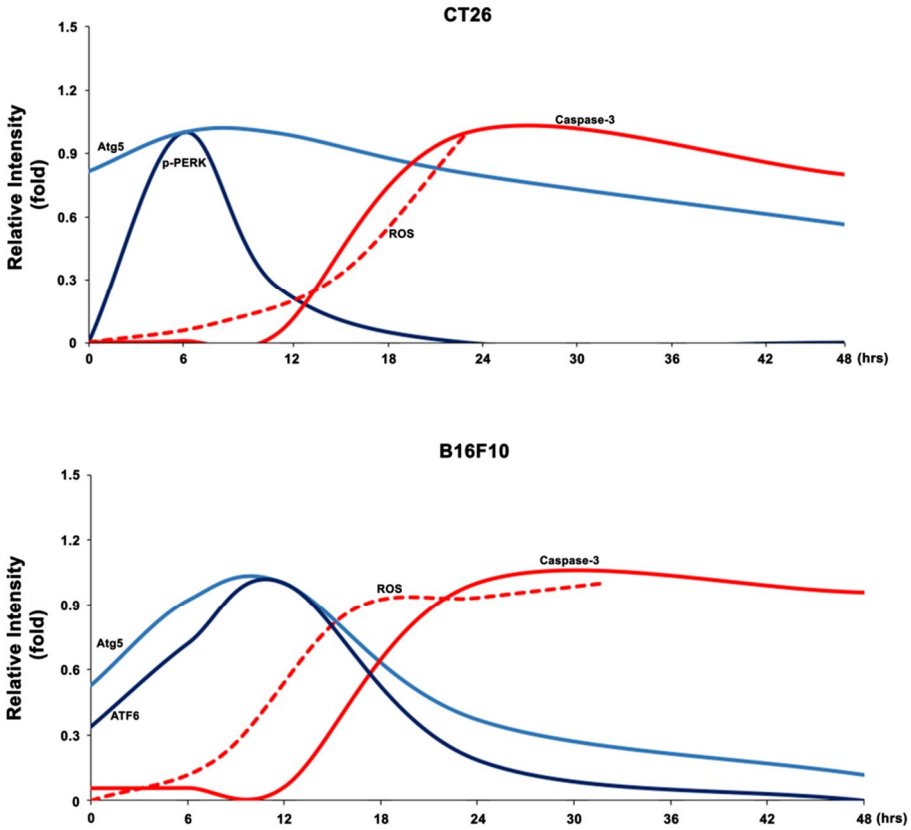

Figure 15. Signal switching from survival to death in bortezomib-treated CT26 and B16F10 cells

Expression levels of each protein from the results of Figure 7 to Figure 9 were analyzed using Image J program. In each case, relative values were calculated on the basis of maximum intensities or scales of activities at 1.

IV. Discussion

Although it has been recognized that signal switch from pro-survival to pro-apoptosis is processed in bortezomib-induced cell death, signal switch occurs too fast to be identified in almost all susceptible cells; over 50% of susceptible cells are dead within 24 hours by addition of bortezomib ranging from 10 nM to 50 nM. Since understanding and controlling of signal switching mechanism could be helpful to solve the therapeutic problems in bortezomib-resistant cells, two moderately resistance cells, CT26 and B16F10 were used to identify mechanism involving in signal switch.

ER stress response has been known as an autophagy inducing mechanism to remove unfolded or misfolded proteins [28, 34]. ER stress response and autophagy were sequentially processed after bortezomib treatment. In CT26 and B16F10 cells, increased ubiquitinated proteins (Figure 9) and ER stress related proteins were detected from 6 hours, and LC3-Ⅱ was detected from 12 hours after bortezomib treatment. Although enzymatic activities of caspase 3 and 8 were increased between 6 and 12 hours after bortezomib treatment respectively, cell death rates were not increased until ER stress response and autophagy were processed. Autophagic flux seemed to be decreased after 24 hours, because activities of caspase 3 and 8 were significantly increased from 24 hours and hence, beclin-1

and Atg5 were decreased at 24 or 48 hours in B16F10 or CT26 cells, respectively. Additionally, ROS was detected from 8 hours and significantly increased 24 hours after bortezomib treatment in CT26 and B16F10 cells. ROS should be a triggering factor for caspase induction as well as a pro-death signal by itself, because caspase 3 activation was reduced by addition of NAC. It could be suggested that accumulation of misfolded or unfolded proteins induced ER stress response and autophagy, which proceeded until ROS increase was enough to induce caspase 3 and 8 activation. Therefore, ER stress response and autophagy were pro-survival signals in these cells. After caspase 3 and 8 activation, beclin-1 and Atg5 were cleaved to inhibit autophagy and induce cell death. It was supported that cell death was reduced by addition of autophagy inhibitors and increased by NAC or caspase inhibitor.

In Figure 15, pattern of signal switch accorded with the conversion model in CT26 cells and the competition model in B16F10 cells, as suggested in previous report [33]. Beclin-1 and Atg5 would be survival indicators in both cells. ROS, caspase 3 and caspase 8 might be death indicators in CT26 cells; ROS and caspase 3 in B16F10 cells. In B16F10 cells, expression pattern of LC3-Ⅰ was similar to those of beclin-1 and Atg5 but LC3-Ⅱ was similar to activated caspase 3. In CT26 cells, expression patterns of LC3-Ⅰ or LC3-Ⅱ were similar to ROS increase. From these results, beclin-1 and Atg5, involved in autophagy

initiation or early phase of phagophore elongation, could be regarded as indicators of survival signals, however LC3-Ⅱ, implicated in late phase of phagophore elongation and autophagosome maturation, could be seen as possible indicators of death signals in bortezomib-treated cells.

V. References

[1] Adams J. The development of proteasome inhibitors as anticancer drugs. Cancer Cell. 2003;5:417-21.

[2] Schroder M, Kaufman RJ. ER stress and the unfolded protein response. Mutat Res. 2005;569(1-2):29-63. doi: 10.1016/j.mrfmmm.2004.06.056. PubMed PMID: 15603751.

[3] Velentzas PD, Velentzas AD, Mpakou VE, Antonelou MH, Margaritis LH, Papassideri IS, et al. Detrimental effects of proteasome inhibition activity in Drosophila melanogaster: implication of ER stress, autophagy, and apoptosis. Cell Biol Toxicol. 2013;29(1):13-37. doi: 10.1007/s10565-012-9235-9. PubMed PMID: 23161111.

[4] Jager R, Bertrand MJ, Gorman AM, Vandenabeele P, Samali A. The unfolded protein response at the crossroads of cellular life and death during endoplasmic reticulum stress. Biol Cell. 2012;104(5):259-70. doi: 10.1111/boc.201100055. PubMed PMID: 22268789.

[5] Iurlaro R, Munoz-Pinedo C. Cell death induced by endoplasmic reticulum stress. FEBS J. 2015. doi: 10.1111/febs.13598. PubMed PMID: 26587781.

[6] Szegezdi E, Logue SE, Gorman AM, Samali A. Mediators of endoplasmic reticulum stress-induced apoptosis. EMBO Rep. 2006;7(9):880-5. doi: 10.1038/sj.embor.7400779. PubMed PMID: 16953201; PubMed Central PMCID: PMCPMC1559676.

[7] Sano R, Reed JC. ER stress-induced cell death mechanisms. Biochim Biophys Acta. 2013;1833(12):3460-70. doi: 10.1016/j.bbamcr.2013.06.028. PubMed PMID: 23850759; PubMed Central PMCID: PMCPMC3834229.

[8] Puthalakath H, O'Reilly LA, Gunn P, Lee L, Kelly PN, Huntington ND, et al. ER stress triggers apoptosis by activating BH3-only protein Bim. Cell. 2007;129(7):1337-49. doi: 10.1016/j.cell.2007.04.027. PubMed PMID: 17604722.

[9] Shiraishi H, Okamoto H, Yoshimura A, Yoshida H. ER stress-induced apoptosis and caspase-12 activation occurs downstream of mitochondrial apoptosis involving Apaf-1. J Cell Sci. 2006;119(Pt 19):3958-66. doi: 10.1242/jcs.03160. PubMed PMID: 16954146.

[10] Julian Adams VJP, Edward A. Sauville, Jill Johnson, Antonia Destress, Douglas D. Lazarus, Jochen Mass, Christine S. Pien, Samuel Prakash, and Peter J. Elliott. Proteasome Inhibitors- A Novel Class of Potent and Effective Antitumor Agents. Cancer Research. 1999;59:2615-22.

[11] Rober C. Kane PFB, Ann T. Farrell, Richard Pazdur. Velcade : U.S. FDA Approval for the Treatment of Multiple Myeloma Progressing on Prior Therapy. The Oncologist. 2003;8:508-13.

[12] Kane RC, Farrell AT, Sridhara R, Pazdur R. United States Food and Drug Administration approval summary: bortezomib for the treatment of progressive multiple myeloma after one prior therapy. Clin Cancer Res. 2006;12(10):2955-60. doi: 10.1158/1078-0432.CCR-06-0170. PubMed PMID: 16707588.

[13] Ling YH, Liebes L, Jiang JD, Holland JF, Elliott PJ, Adams J, et al. Mechanisms of proteasome inhibitor PS-341-induced G(2)-M-phase arrest and apoptosis in human non-small cell lung cancer cell lines. Clin Cancer Res. 2003;9(3):1145-54. PubMed PMID: 12631620.

[14] Bonvini P, Zorzi E, Basso G, Rosolen A. Bortezomib-mediated 26S proteasome inhibition causes cell-cycle arrest and induces apoptosis in CD-30+ anaplastic large cell lymphoma. Leukemia. 2007;21(4):838-42. doi: 10.1038/sj.leu.2404528. PubMed PMID: 17268529.

[15] Hong YS, Hong SW, Kim SM, Jin DH, Shin JS, Yoon DH, et al. Bortezomib induces G2-M arrest in human colon cancer cells through ROS-inducible phosphorylation of ATM-CHK1. Int J Oncol. 2012;41(1):76-82. doi: 10.3892/ijo.2012.1448. PubMed PMID: 22552540.

[16] Adams J. The proteasome as a novel target for the treatment of breast cancer. Breast Dis. 2002;15:61-70. PubMed PMID: 15687646.

[17] Richardson PG, Anderson KC. Bortezomib: a novel therapy approved for multiple myeloma. Clin Adv Hematol Oncol. 2003;1(10):596-600. PubMed PMID: 16258456.

[18] Belloni D, Veschini L, Foglieni C, Dell'Antonio G, Caligaris-Cappio F, Ferrarini M, et al. Bortezomib induces autophagic death in proliferating human endothelial cells. Exp Cell Res. 2010;316(6):1010-8. doi: 10.1016/j.yexcr.2009.11.005. PubMed PMID: 19917281.

[19] Rajkumar SV, Richardson PG, Hideshima T, Anderson KC. Proteasome inhibition as a novel therapeutic target in human cancer. J Clin Oncol. 2005;23(3):630-9. doi: 10.1200/JCO.2005.11.030. PubMed PMID: 15659509.

[20] Jackson G, Einsele H, Moreau P, Miguel JS. Bortezomib, a novel proteasome inhibitor, in the treatment of hematologic malignancies. Cancer Treat Rev. 2005;31(8):591-602. doi: 10.1016/j.ctrv.2005.10.001. PubMed PMID: 16298074.

[21] Baradari V, Hopfner M, Huether A, Schuppan D, Scherubl H. Histone deacetylase inhibitor MS-275 alone or combined with bortezomib or sorafenib exhibits strong antiproliferative action in human cholangiocarcinoma cells. World J Gastroenterol. 2007;13(33):4458-66. PubMed PMID: 17724801; PubMed Central PMCID: PMCPMC4611578.

[22] Demo SD, Kirk CJ, Aujay MA, Buchholz TJ, Dajee M, Ho MN, et al. Antitumor activity of PR-171, a novel irreversible inhibitor of the proteasome. Cancer Res. 2007;67(13):6383-91. doi: 10.1158/0008-5472.CAN-06-4086. PubMed PMID: 17616698.

[23] Yerlikaya A, Okur E, Eker S, Erin N. Combined effects of the proteasome inhibitor bortezomib and Hsp70 inhibitors on the B16F10 melanoma cell line. Mol Med Rep. 2010;3(2):333-9. doi: 10.3892/mmr_00000262. PubMed PMID: 21472244.

[24] Wunderlich A, Arndt T, Fischer M, Roth S, Ramaswamy A, Greene BH, et al. Targeting the proteasome as a promising therapeutic strategy in thyroid cancer. J Surg Oncol. 2012;105(4):357-64. doi: 10.1002/jso.22113. PubMed PMID: 22006286.

[25] Niesvizky R, Badros AZ, Costa LJ, Ely SA, Singhal SB, Stadtmauer EA, et al. Phase 1/2 study of cyclin-dependent kinase (CDK)4/6 inhibitor palbociclib (PD-0332991) with bortezomib and dexamethasone in relapsed/refractory multiple myeloma. Leuk Lymphoma. 2015;56(12):3320-8. doi: 10.3109/10428194.2015.1030641. PubMed PMID: 25813205.

[26] Moore BS, Eustáquio AS, McGlinchey RP. Advances in and applications of proteasome inhibitors. Current Opinion in Chemical Biology. 2008;12(4):434-40. doi: 10.1016/j.cbpa.2008.06.033.

[27] Yue Y, Wang Y, He Y, Yang S, Chen Z, Wang Y, et al. Reversal of bortezomib resistance in myelodysplastic syndrome cells by MAPK inhibitors. PLoS One. 2014;9(3):e90992. doi: 10.1371/journal.pone.0090992. PubMed PMID: 24608798; PubMed Central PMCID: PMCPMC3946707.

[28] Galluzzi L B-SPJ, Vitale I, Aaronson SA, Abrams JM, Adam D, Alnemri ES, Altucci L, Andrews D, Annicchiarico-Petruzzelli M, Baehrecke EH, Bazan NG, Bertrand MJ, Bianchi K, Blagosklonny MV, Blomgren K, Borner C, Bredesen DE, Brenner C, Campanella M, Candi E, Cecconi F, Chan FK, Chandel NS, Cheng EH, Chipuk JE, Cidlowski JA, Ciechanover A, Dawson TM, Dawson VL, De Laurenzi V, De Maria R, Debatin KM, Di Daniele N, Dixit VM, Dynlacht BD, El-Deiry WS, Fimia GM, Flavell RA, Fulda S, Garrido C, Gougeon ML, Green DR, Gronemeyer H, Hajnoczky G, Hardwick JM, Hengartner MO, Ichijo H, Joseph B, Jost PJ, Kaufmann T, Kepp O, Klionsky DJ, Knight RA, Kumar S, Lemasters JJ, Levine B, Linkermann A, Lipton SA, Lockshin RA, López-Otín C, Lugli E, Madeo F, Malorni W, Marine JC, Martin SJ, Martinou JC, Medema JP, Meier P, Melino S, Mizushima N, Moll U, Muñoz-Pinedo C, Nuñez G, Oberst A, Panaretakis T, Penninger JM, Peter ME, Piacentini M, Pinton P, Prehn JH, Puthalakath H, Rabinovich GA, Ravichandran KS, Rizzuto R, Rodrigues CM, Rubinsztein DC, Rudel T, Shi Y, Simon HU, Stockwell BR, Szabadkai G, Tait SW, Tang HL, Tavernarakis N, Tsujimoto Y, Vanden Berghe T, Vandenabeele P, Villunger A, Wagner EF, Walczak H, White E, Wood WG, Yuan J, Zakeri Z, Zhivotovsky B, Melino G, Kroemer G. Essential versus accessory aspects of cell death: recommendations of the NCCD 2015. Cell death and Differentiation. 2015;22(1):58-73.

[29] Gernot Stuhler TSN. Myeloma cell sensitivity to bortezomib is associated with Dicer1 expression. Blood. 2014;124(24):657-8.

[30] Hiromasa Hdeshima YY, Hiroshi Ikeda, Maya Hide, Akinori Iwasaki, Keneth C. Anderson and Teru Hideshma. IKKβ inhibitor in combination with bortezomib induces cytotoxicity in breast cancer cells. International Journal of Oncology. 2014;44(4):1171-6.

[31] Paul G. Richardson TH, and Kenneth C. Anderson, MD. Bortezomib (PS-341): A Novel, First-in-Class Proteasome Inhibitor for the Treatment of Multiple Myeloma and Other Cancers. Cancer Control. 2003;10(5):361-9.

[32] Criollo A, Maiuri MC, Tasdemir E, Vitale I, Fiebig AA, Andrews D, et al. Regulation of autophagy by the inositol trisphosphate receptor. Cell Death Differ. 2007;14(5):1029-39. doi: 10.1038/sj.cdd.4402099. PubMed PMID: 17256008.

[33] Hoyer-Hansen M, Jaattela M. Connecting endoplasmic reticulum stress to autophagy by unfolded protein response and calcium. Cell Death Differ. 2007;14(9):1576-82. doi: 10.1038/sj.cdd.4402200. PubMed PMID: 17612585.

[34] Kroemer G, Marino G, Levine B. Autophagy and the integrated stress response. Mol Cell. 2010;40(2):280-93. doi: 10.1016/j.molcel.2010.09.023. PubMed PMID: 20965422; PubMed Central PMCID: PMCPMC3127250.

[35] Mukhopadhyay S, Panda PK, Sinha N, Das DN, Bhutia SK. Autophagy and apoptosis: where do they meet? Apoptosis. 2014;19(4):555-66. doi: 10.1007/s10495-014-0967-2. PubMed PMID: 24415198.

[36] Chen HI, Tsai HP, Chen YT, Tsao SC, Chai CY. Autophagy and Apoptosis Play Opposing Roles in Overall Survival of Esophageal Squamous Cell Carcinoma. Pathol Oncol Res. 2016. doi: 10.1007/s12253-016-0051-z. PubMed PMID: 26980476.

[37] Shah SA, Potter MW, McDade TP, Ricciardi R, Perugini RA, Elliott PJ, et al. 26S proteasome inhibition induces apoptosis and limits growth of human pancreatic cancer. J Cell Biochem. 2001;82(1):110-22. PubMed PMID: 11400168.

[38] Yu C, Rahmani M, Conrad D, Subler M, Dent P, Grant S. The proteasome inhibitor bortezomib interacts synergistically with histone deacetylase inhibitors to induce apoptosis in Bcr/Abl+ cells sensitive and resistant to STI571. Blood. 2003;102(10):3765-74. doi: 10.1182/blood-2003-03-0737. PubMed PMID: 12893773.

[39] Lipchick BC, Fink EE, Nikiforov MA. Oxidative stress and proteasome inhibitors in multiple myeloma. Pharmacol Res. 2016;105:210-5. doi: 10.1016/j.phrs.2016.01.029. PubMed PMID: 26827824.

[40] Galluzzi L, Bravo-San Pedro JM, Vitale I, Aaronson SA, Abrams JM, Adam D, et al. Essential versus accessory aspects of cell death: recommendations of the NCCD 2015. Cell Death Differ. 2015;22(1):58-73. doi: 10.1038/cdd.2014.137. PubMed PMID: 25236395; PubMed Central PMCID: PMCPMC4262782.

[41] Caitriona Holohan SVS, Daniel B. Longle & Patrick G. Johnston Cancer drug resistance: an evolving paradigm. Nature reviews cancer. 2013;13:714-26.

[42] Stephanie Markovina NSC, Shelby L O'Connor, Jihoon Kim, Jae E Werndli, Martha Raschko, Catherine P Leith, Brad S Kahl, KyungMann Kim and Shigeki Miyamoto. Bortezomib-Resistant NF-κB Activity in Multiple Myeloma Cells. Molecular Cancer research. 2008;6(8):1356-64.

[43] Wang SLaJ. The resistance mechanisms of proteasome inhibitor bortezomib. Biomarker Research. 2013;1(13).

[44] Tsubuki S SY, Tomioka M, Ito H, Kawashima S. Differential inhibition of calpain and proteasome activities by peptidyl aldehydes of di-leucine and tri-leucine. The Journal of Biochemistry. 1996;119(3):572-6.

[45] Kuhn DJ CQ, Voorhees PM, Strader JS, Shenk KD, Sun CM, Demo SD, Bennett MK, van Leeuwen FW, Chanan-Khan AA, Orlowski RZ. Potent activity of carfilzomib, a novel, irreversible inhibitor of the ubiquitin-proteasome pathway, against preclinical models of multiple myeloma. Blood. 2007;110(9):3281-90.

[46] Kupperman E LE, Cao Y, Bannerman B, Fitzgerald M, Berger A, Yu J, Yang Y, Hales P, Bruzzese F, Liu J, Blank J, Garcia K, Tsu C, Dick L, Fleming P, Yu L, Manfredi M, Rolfe M, Bolen J. Evaluation of the proteasome inhibitor MLN9708 in preclinical models of human cancer. Cancer Research. 2010;70(5):1970-80.

[47] Zhou HJ AM, Bennett MK, Dajee M, Demo SD, Fang Y, Ho MN, Jiang J, Kirk CJ, Laidig GJ, Lewis ER, Lu Y, Muchamuel T, Parlati F, Ring E, Shenk KD, Shields J, Shwonek PJ, Stanton T, Sun CM, Sylvain C, Woo TM, Yang J. Design and synthesis of an orally bioavailable and selective peptide epoxyketone proteasome inhibitor (PR-047). Journal of Medicinal Chemistry. 2009;52(9):3028-38.

[48] Richardson PG. Update on Proteasome Inhibitors in Multiple Myeloma. Hematology and Oncology. 2014;12(3).

[49] Lenka Kubiczkova LP, Lenka Sedlarikova, Roman Hajek and Sabina Sevcikova. Proteasome inhibitors – molecular basis and current perspectives in multiple myeloma. Journal of Cellular and Molecular Medicine. 2014;18(6):947-61.

[50] andZihaiLi B. Endoplasmicreticulum stress in hepaticsteatosis and inflammatory bowel diseases. Frontiers in Genetics. 2014;5.

[51] Asaha Fujimoto KK, Ayumi Taguchi, Katsuyuki Adachi, Masakazu, Sato HN, Juri Ogishima, Mitsuyo Yoshida, Tomoko Inoue,, Haruka Nishida KT, Aki Yamashita, Yoko Matsumoto, Takahide, Arimoto OW-H, Katsutoshi Oda, Takeshi Nagamatsu, Yutaka, Osuga TF. Inhibition of endoplasmic reticulum (ER) stress sensors sensitizes cancer stem-like cells to ER stress-mediated apoptosis. Oncotarget. 2016;7(32).

[52] Esther A. Obeng LMC, Delia M. Gutman, William J. Harrington Jr, Kelvin P. Lee, and Lawrence H. Boise. Proteasome inhibitors induce a terminal unfolded protein response in multiple myeloma cells. Blood. 2006;107:4907-16. doi: 10.1182/.

[53] Yamaguchi H, Wang HG. CHOP is involved in endoplasmic reticulum stress-induced apoptosis by enhancing DR5 expression in human carcinoma cells. J Biol Chem. 2004;279(44):45495-502. doi: 10.1074/jbc.M406933200. PubMed PMID: 15322075.

[54] Liu X, Yue P, Chen S, Hu L, Lonial S, Khuri FR, et al. The proteasome inhibitor PS-341 (bortezomib) up-regulates DR5 expression leading to induction of apoptosis and enhancement of TRAIL-induced apoptosis despite up-regulation of c-FLIP and survivin expression in human NSCLC cells. Cancer Res. 2007;67(10):4981-8. doi: 10.1158/0008-5472.CAN-06-4274. PubMed PMID: 17510429.

[55] McCullough KD, Martindale JL, Klotz LO, Aw TY, Holbrook NJ. Gadd153 sensitizes cells to endoplasmic reticulum stress by down-regulating Bcl2 and perturbing the cellular redox state. Mol Cell Biol. 2001;21(4):1249-59. doi: 10.1128/MCB.21.4.1249-1259.2001. PubMed PMID: 11158311; PubMed Central PMCID: PMCPMC99578.

[56] Kaufman KZRJ. Review Article From endoplasmic-reticulum stress to the inflammatory response. Nature. 2008;454:455-62.

[57] Jyoti D. Malhotra HM, Kezhong Zhang, Anna Wolfson, Subramaniam Pennathur, Steven W. Pipe, and Randal J. Kaufmana. Antioxidants reduce endoplasmic reticulum stress and improve protein secretion. Proceedings of the National Academy of Sciences of the United States of America. 2008;05(47):18525-39.

[58] Atsushi Masui MH, Hiroyasu Kameyama, Ken Wakabayashi, Ayako Takasu, Tomoaki Imai, Soichi Iwai, Yoshiaki Yura. Autophagy as a Survival Mechanism for Squamous Cell Carcinoma Cells in Endonuclease G-Mediated Apoptosis. PLoS one. 2016;11(9).